Food and Bioproducts Processing 154 (2025) 392–401

Contents lists available at ScienceDirect

Food and Bioproducts Processing

journal homepage: www.elsevier.com/locate/fbp

Parameter optimization of drying models using Honey Formation Optimization-1 (HFO-1)

Uğur Ercan [a], Ismail Boyar [b], Tugce Ozsan Kilic [c], Zeki Yetgin [d], Can Ertekin [b,*]

[a] Department of Informatics, Akdeniz University, Antalya 07070, Türkiye
[b] Department of Agricultural Machinery and Technologies Engineering, Faculty of Agriculture, Akdeniz University, Antalya 07070, Türkiye
[c] Department of Horticulture, Faculty of Agriculture, Akdeniz University, Antalya 07070, Türkiye
[d] Department of Computer Engineering, Faculty of Engineering, Mersin University, Mersin 33100, Türkiye

ARTICLE INFO

Keywords:
Drying
Modeling
Bitter Gourd
HFO-1
GA
PSO

ABSTRACT

Many mathematical studies in recent years has been proposed to model the drying curves for various grains, fruits and vegetables. In this study, one of the recent optimization algorithms, Honey Formation Optimization with single component (HFO-1) and also Genetic Algorithm (GA) and Particle Swarm Optimization (PSO) are utilized to model the drying curves of the bitter gourd (*Momordica charantia* L.). For this purpose, the bitter gourd was sliced in 8 mm slice thickness and dried at 70°C drying air temperature in convective dryer by applying different pre-treatments such as dipping time (10, 20 and 30 h) and different sugar and grape molasses content (pekmez) (50, 60 and 70 Brix). During the drying period, weight measurements are recorded until the products reached equilibrium moisture content. The values are obtained from 14 commonly used thin layer drying models. The results show that the HFO-1 is observed to perform better than GA and PSO in optimizing the parameters of each thin layer drying models. With HFO-1, the Modified Henderson and Pabis I and II are found to provide better results with respect to RMSE, χ^2, MAE and EF metrics. The best RMSE, χ^2, MAE and EF values are achieved in the Modified Henderson and Pabis I model with a value of 5.74E-04, 4.43E-07, 4.08E-04 and 1.00E+ 00, respectively, for the samples dipped in 70 Brix sugar for 10 h. With respect to the lowest RMSE values achieved, HFO-1 is observed to perform at least 6.84E+ 02 % better than the both PSO and GA. Altogether, this study presents three contributions. First, it introduces the novel use of the recently developed HFO-1 algorithm to optimize thin-layer drying models—a context in which this algorithm has not been previously applied. Second, these 14 drying models, along with their associated pre-treatments, are collectively applied for the first time to bitter gourd fruit.Third, it provides a robustness evaluation of the drying model against noisy data, enhancing their reliability for practical use. The findings of this study enable significant advancements, including more accurate prediction of drying time and shelf life, improved process optimization and control, enhanced design of efficient drying systems, and strengthened efforts toward final product quality and standardization.

1. Introduction

Many studies have shown that consumption of fruits and vegetables reduces the chance of developing various degenerative diseases such as heart disease and some types of cancer (Stanner et al., 2004; Giampieri et al., 2014). It is widely known that phytochemicals, especially those with antioxidant capacity, contribute to the general health-protective properties of fruits and vegetables by attenuating the effects of oxidative stress on disease development and the aging process (Alvarez-Suarez et al., 2014). One of the oldest food preservation methods still used today is drying, an important component of the food processing industry. It is a method used for the preservation of grains, fruits, vegetables, herbs and other products, as it has a significant effect on reducing shipping weights, reducing packaging costs and extending the shelf life of fresh foods (Hamrouni-Sellami et al., 2011; Rajkumar et al., 2017).

One of the pretreatments applied to preserve the volatile chemicals of the products, improve the drying kinetics and preserve the physical and nutritional qualities of the products is the osmotic drying process (Sharma and Varma, 2014). The product loses water as a result of

* Corresponding author.
E-mail addresses: ugurercan@akdeniz.edu.tr (U. Ercan), ismailboyar@akdeniz.edu.tr (I. Boyar), tugceozsan@akdeniz.edu.tr (T.O. Kilic), zyetgin@mersin.edu.tr (Z. Yetgin), ertekin@akdeniz.edu.tr (C. Ertekin).

https://doi.org/10.1016/j.fbp.2025.09.016
Received 22 July 2024; Received in revised form 20 August 2025; Accepted 19 September 2025
Available online 2 October 2025
0960-3085/© 2025 Institution of Chemical Engineers. Published by Elsevier Ltd. All rights are reserved, including those for text and data mining, AI training, and similar technologies.

immersion in a hypertonic solution (which has an osmotic pressure greater than the cell itself). This solution fills the space between the cell wall and the plasmalemma since the cell wall is porous (Lewicki and Lenart, 2006). High hydrostatic pressure and osmotic dehydration cause the cells to dehydrate while absorbing soluble solids until equilibrium is reached, at which point the net transport phenomenon becomes insignificant.

Pretreatments with sugar and brine shorten the drying process and increase the storage capacity of the final product (Zzaman et al., 2021; Roy et al., 2022). They use less energy, prevent both enzymatic and non-enzymatic browning processes, and preserve odor and color as well as remove intercellular and surface gases to prevent oxidation, discoloration, softening, and off-flavor development (Hossain et al., 2021).

Some studies have shown that the use of osmotic pretreatment immersion solution increases the nutritional benefits of the product due to its high natural sugar content and at the same time reduces the processing cost by limiting the amount of sucrose added to the osmotic solution (Bchir et al. 2012). Grape product 'Pekmez' (grape molasses), which has rich components for human health, is created by boiling grape juices to a soluble solids concentration of approximately 70 %. Molasses, a healthy food obtained without the use of sugar or other sweeteners, is preferred by children, athletes and those who need a quick energy boost due to its high sugar, mineral and organic acid content.

Bitter gourd (Momordica charantia L.), a valuable vegetable from the Cucurbitaceae family used in this study, is a product known for its health properties such as anti-inflammatory, anti-cancer, anti-ulcer, antiviral and anti-osteoporosis properties (Jin et al., 2019). Its chemical components and bioactive compounds contain pharmacological properties (Yan et al., 2019). Due to its high moisture content, fresh bitter gourd fruits are prone to spoilage like other agricultural products used in horticulture. The amounts of phenolic compounds and antioxidant components in such products are affected by different preservation methods. Bitter gourd is perishable and only available in certain seasons; therefore, it needs to be preserved. Preservation should be done appropriately and carefully to minimize biodegradation, preserve the natural characteristics of the fresh product as much as possible and maximize the chance of its availability over many seasons (Mehta et al., 2017; Jin et al., 2019). By removing acid and absorbing osmotic solutions such as sugar and grape molasses, osmotic pretreatment improves the color, odor, nutrient content and flavor component retention value of fruits and vegetables in addition to their shelf life. As a result, fruits and vegetables are sweeter and less bitter than non-osmotic dried products. The market value of pretreated products can be increased and production can be optimized by applying osmotic pretreatment. Therefore, there is a high possibility of increased utilization of dried bitter gourd (Yadav and Singh, 2014; Kudri et al., 2022).

In order to predict moisture ratio models' coefficients, non-linear regression analysis by LAB Fit Curve Fitting Software for hot air drying of banana (Da Silva et al., 2014). Another study for hot air drying of Mentha haplocalyx leaves by using Originlab (Guo et al., 2022). Curve fitting techniques in MATLAB in microwave drying of beetroot (Ahmed et al., 2023) and insolar drying of potato (Singh et al., 2023) and in convective drying of potato (Tepe, 2023a) and banana (Tepe, 2023b) and in infrared drying of garlic (Ardabili et al., 2023). This method is evaluated for convective drying of apple (Hamdani et al., 2006), for thyme leaves (Turan and Firatligil, 2019). STATGRAPHICS Software also used for convective drying of burdock root (Nguyen et al., 2023a). For non-linear regression analysis of convective drying of potato, MINITAB is used (Erol, 2022). Using Levenberg-Marquardt procedure in Sigmaplot by nonlinear least square regression analysis is applied in vacuum drying of olive pomace (Maamar et al., 2023). Sigmaplot software is used in convective drying of potato peel (Nguyen et al., 2023b) and black pepper (Jayashree and Zachariah, 2022). STATISTICA Software developed by SPSS 18 is used for convective drying of jujube (Yi et al., 2012) and in fluidized bed drying of Moringa leaves (Ambawat et al., 2022). Curve Expert used for convective drying of sweet potato (Kamal et al., 2023). In solar drying of fig, Curve Expert and Originpro is used (Hssaini et al., 2021). SPSS Software is used for drying of tomato in convective dryer (Taheri-Garavand et al., 2011). Non-linear regression using solver tool in MSExcel is used in microwave drying of Jaya fish (Ghimire et al., 2020). SPSS and MSExcel used for convective drying of cassava chips (Argo et al., 2018).

Metaheuristic methods are algorithms used to solve optimization problems and can provide near-optimal solutions in a reasonable time. These algorithms have been widely used in science and engineering for solving complex problems (Abualigah et al., 2022; Karimi-Mamaghan et al., 2022; Yang et al., 2023). Recent advancements have also seen the rise of sophisticated techniques like metalearning-based algorithms, which have shown promise in solving complex nonconvex optimization problems, further highlighting the trend towards intelligent, data-driven approaches in engineering (Xia et al., 2023). There are many metaheuristic algorithms proposed by researchers in recent years. These can be roughly divided into four parts; Swarm intelligence, Physics-based, Evolutionary, Human-inspired algorithms (Wen et al., 2022; Jia et al., 2023). A honey formation optimization framework (HFO) has been presented recently for design challenges. For numerical optimization problems, this framework presupposes that the objective function formula is known or is in the process of being designed (Yetgin and Abaci, 2021; Yetgin and Samdan, 2021). HFO uses the idea of numerous components in a source to represent the first stage of honey generation within the bee. These commonly used 14 different moisture ratio model were firstly applied for bitter gourd. HFO-1, in contrast to HFO, does not require knowledge of the objective function's formula in advance (Yetgin and Ercan, 2023). The motivation for selecting HFO-1 over more traditional metaheuristics stems from its advantages in fast convergence and success in low-dimensional search spaces. Its use of a random walk behavior allows it to update multiple dimensions of a solution simultaneously, potentially avoiding local optima where other algorithms might falter. In this study, the mathematical models, Newton, Henderson and Pabis, Page, Two-term, Modified Henderson and Pabis I, Modified Henderson and Pabis II, Midilli et al., Verma et al., Alibas et al., Haghi and Andiz, Demir et al., Midilli and Kucuk, Yun et al. and Hii et al. models for moisture ratio are used and the parameters of each model were optimized using the HFO-1 algorithm. Although HFO-1 is used to solve some optimization problems in literature, this study is the first to apply HFO-1 to determine the parameters of thin-layer drying models. Moreover, this study also demonstrates HFO-1 performance superiority with respect to the classical algorithms GA and PSO in this context.

2. Material and methods

2.1. Material, sample preparation and drying tests

Bitter gourd, scientifically known as Momordica charantia, is a green, cucumber-shaped vegetable with a distinctively bitter taste. Commonly used in various culinary traditions, particularly in Asian cuisines, it is prized for its unique flavor profile and potential health benefits. Despite its intense bitterness, bitter gourd is valued for its rich nutritional content and is often incorporated into dishes, both for its taste and reputed medicinal properties (Kumar and Bhowmik, 2010).

Medium size bitter gourds, characterized by ripeness in color and softness, were harvested from a private garden in the Antalya region (36°53'10.1" N 30°45'23.4" E). To ensure their preservation, the bitter gourds were carefully stored in separate boxes and transported to the laboratories of Akdeniz University. Subsequent to harvesting, the bitter gourds underwent a cleaning process involving washing with tap water and drying with towels. The gourds were then sliced into thicknesses of 8 mm (Ozsan Kilic et al., 2023a). Slices that did not attain a uniform ring form during the slicing process were set aside for further treatment. The seeds within the sliced fruits and the red pulp around the seeds were meticulously cleaned. The sliced bitter gourd samples underwent a blanching process by dipping 93.5°C distilled water for 5 min, they were

taken to 4°C distilled water (water to ice ratio of 4:1) and the scalding process was stopped. With this process, it is aimed to inactivate the enzymes in the bitter gourd to halt the heating stage and then drained for 1 min (Ertekin and Heybeli, 2014; Mehta et al., 2017). The initial weights of the sliced products were measured, and mixtures with varying Brix values (50−60−70) were created for sugar (S) and grape molasses (G) pre-treatment applications. The fruit-to-mixture ratio was set at ¼. Control group (NP) samples did not undergo any blanching but were dried. All sliced bitter gourds, including the control group, were weighed and positioned on drying trays (Ozsan Kilic et al., 2023b).

The drying process was conducted using a 12-shelf, horizontal airflow, 1000 Watt cabinet convective dryer (Dalle, LT-27, Türkiye). The convective dryer could be adjusted to drying air temperatures ranging from 30°C to 90°C with 5°C differences, and it featured a 24-hour adjustable timer (Hazar et al., 2023). The experiments were executed at drying air temperatures of 70°C, with a constant air velocity of 1.5 m/s, and weight measurements were taken at 15-minute intervals. The trials concluded when the moisture content had decreased to 10 % or below, as determined by the measurements. The moisture content of the fresh samples was determined by drying at 105°C for 24 h (Akman et al., 2022).

2.2. Mathematical modeling of drying process

The moisture ratio (MR) data for the samples, as outlined in Eq. 1, was subjected to analysis using the 14 different models (Newton, Henderson and Pabis, Page, Two-term, Modified Henderson and Pabis I, Modified Henderson and Pabis II, Midilli et al., Verma et al., Alibas et al., Haghi and Andiz, Demir et al., Midilli and Kucuk, Yun et al. and Hii et al.) presented in Table 1. Although there are more than hundred thin layer drying model, only widely and commonly used models were evaluated in this study (Ertekin and Firat, 2017). The parameters for all models were determined utilizing the implementation of HFO-1 in Matlab™. To assess the effectiveness of the models, the root mean square error (RMSE), Chi-square (χ^2), modeling efficiency (EF) and mean absolute error (MAE), as defined in Eqs. 2–5, was employed. The calculation of these parameters was conducted in accordance with the provided equations (Parisotto et al., 2020; Ertekin and Firat, 2017; Doymaz, 2009; Shahhoseini et al., 2013; Cai et al., 2015; Polat and Izli, 2022; Balbay and Sahin., 2012). Throughout the drying processes, the moisture ratio (MR) of the samples was computed based on Eq. 1.

$$MR = \frac{M_t - M_e}{M_0 - M_e} \tag{1}$$

$$RMSE = \sqrt{\frac{1}{N}\sum_{i=1}^{N}\left(MR_{pre,i} - MR_{\exp,i}\right)^2} \tag{2}$$

$$\chi^2 = \frac{\sum_{i=1}^{N}\left(MR_{pre,i} - MR_{\exp,i}\right)^2}{N - n} \tag{3}$$

$$EF = \frac{\sum_{i=1}^{N}\left(MR_{\exp,i} - MR_{\exp,ave}\right)^2 - \sum_{i=1}^{N}\left(MR_{pre,i} - MR_{\exp,i}\right)^2}{\sum_{i=1}^{N}\left(MR_{\exp,i} - MR_{\exp,ave}\right)^2} \tag{4}$$

$$MAE = \frac{1}{N}\sum_{i=1}^{N}\left|MR_{\exp,i} - MR_{pre,i}\right| \tag{5}$$

Table 1
Selected drying models for describing experimental drying data.

Model name	Model equation	Reference
Newton	$MR = \exp(-kt)$	Yaldız and Ertekin, 2001
Henderson and Pabis	$MR = a\exp(-kt)$	Kayisoglu and Ertekin, 2011
Page	$MR = \exp(-kt^n)$	Ertekin and Firat, 2017
Two-term	$MR = a\exp(-k_0 t) + b\exp(-k_1 t)$	Delgado et al., 2014
Modified Henderson and Pabis I	$MR = a\exp(-kt) + b\exp(-gt) + c\exp(-ht)$	Arslan and Ozcan, 2012
Modified Henderson and Pabis II	$MR = a\exp(-kt^n) + b\exp(-gt) + c\exp(-ht)$	Corzo et al., 2011
Midilli et al.	$MR = a\exp(-kt^n) + bt$	Midilli et al., 2002
Verma et al.	$MR = a\exp(-kt) + (1-a)\exp(-gt)$	Karaaslan et al., 2021
Alibas et al.	$MR = a\exp[(-kt^n) + bt] + g$	Alibas, 2012
Haghi and Angiz	$MR = a\exp(-bt^c) + dt^2 + et + f$	Haghi and Angiz, 2007
Demir et al.	$MR = a\exp(-kt^n) + c$	Demir et al., 2007
Midilli and Kucuk	$MR = a\exp(-k_1 t^n) - \exp(-k_2 t^n) - bt^n$	Midilli and Kucuk, 2023
Yun et al.	$MR = \frac{a + bt + ct^2}{1 + dt + ft^2}$	Yun et al., 2013
Hii et al.	$MR = a\exp(-kt^n) + c\exp(-gt^n)$	Hii et al., 2009

t: drying time (min); MR: moisture ratio, k, a, b, c, d, e, f, g, h, n, k_0, k_1, k_2 are model constants.

2.3. HFO-1 algorithm and its application to moisture ratio models

Honey Formation Optimization for Single Component, shortly HFO-1, is a swarm-based optimization algorithm, introduced by Yetgin and Ercan (Yetgin and Ercan, 2023). It is developed for numerical function optimization problems where the formula of the objective function is not explicitly required. HFO-1 attempts to model the honey production processes of the bees. HFO-1 inherits the honey formation process from HFO framework, which is considered as individual mixing process inside the foraging bees and introduces additional mixing processes for honey production, such as collaborative mixing and saturation in the hive. Unlike the artificial bee colony variants, which model the foraging behaviors of honey bees, HFO-1 models the honey production process with 5 phases, initialization, honey formation, mixing, maturation and saturation. The skeleton of the HFO-1 algorithm is shown in Scheme 1.

With the initialization phase, the algorithm starts with a randomly generated set of candidate solutions, which are the raw honey-forms. The honey formation phase is the exploit phase of the honey bee where the bee mixes the visited foods with its own enzymes and the personal mixture mature overtime. This phase is also called mixing-0. When the bees have sufficient honey formation they mix their personal mixtures among themselves in the hive by sharing via sessions, called mixing-1 and mixing-2, which corresponds to chewing and spitting cycles from one mouth to the other. With the maturation phase, the mixture of the honey-forms becomes homogenous enough so that a new mixture is initialized from a new zone and the "Gbest" is used as catalyzer for subsequent productions. The algorithm checks the maturation status of the honey at regular intervals. The maturation phase is observed when all forms of honey are homogeneous with "Pbest" and "Gbest" cannot be improved for some period. However, if the "Gbest" cannot be improved for a long period, despite changing zones, saturation phase starts to finalize the whole honey production process. You can find detailed information about the HFO-1 algorithm in the study conducted by Yetgin and Ercan (Yetgin and Ercan, 2023).

In the context of optimizing the drying moisture ratio model, the model parameters make up the honey-form (solution) in the form of vector and the mean square error between the model outputs and the empirical outputs over drying period is used as objective function.

The default parameters of HFO-1 algorithm are used as suggested by Yetgin and Ercan (Yetgin and Ercan, 2023) for the experiments. The suggested parameters of PSO (Mirjalili, 2024a) and GA (Mirjalili,

HFO-1 Skeleton

```
Sources ← initialize_honey_sources
Gbest ← Pbest ← Sources[1]
repeat
    for each source of workers
        component ← source
        Sources ← exploit(source, component)
    for each onlooker
        source ← select_a_source(Sources)
        Sources ← exploit(source)
    if mixing phase
        Sources ← mix honey-forms with PBest and others randomly
    ensure the Pbest form is not corrupted
    if maturation phase
        Sources ← initialize_honey_sources and set newSite = true
    else if saturation phase
        Sources[mx] ← Pbest ← Gbest with random mx and set newSite = false
    if Gbest is not improved for one maturation period
        change mixing sizes randomly
until maximum iteration
```

Scheme 1. Skeleton of the HFO-1 algorithm.

2024b) are used as implemented in Mirjalili's works. Metaheuristic optimization algorithms perform their searches within a certain range in the search space when determining parameter values. This range varies depending on the problem. Although many ranges have been tried in the study, the best values are generally observed with the parameter values in the [-1, 4] range. Initial parameters of GA, HFO-1, and PSO algorithms are shown in Table 2.

3. Results and discussion

Within the scope of the study, after bitter gourd slices were dried at different brix values (50, 60, 70 Brix) and for different dipping times (10, 20, 30 h) and dipped into sugar and grape molases, they were examined with 14 different thin layer drying models (Newton, Henderson and Pabis, Page, Two-term, Modified Henderson and Pabis I, Modified Henderson and Pabis II, Midilli et al., Verma et al., Alibas et al., Haghi and Andiz, Demir et al., Midilli and Kucuk, Yun et al. and Hii et al.) with different algorithms as HFO-1, GA and PSO algorithms. The first three best models according to the statistical criteria were given in Table 3. According to the results of the comparison of different algorithms, the worst statistical values obtained by using GA algorithm. While the RMSE, χ^2 and MAE values were very high compared the others, EF values were very low with GA algorithm. When HFO-1 and PSO algorithms compared, in some dipping times and pre-treatment applications, the statistical values are very close to each other, but in general HFO-1 algorithm gave better results (Fig. 1). So, the best models coefficients obtained by HFO-1 algorithm with statistical criteria of RMSE, χ^2, MAE and EF values were given in Table 4.

Table 2
Initial Parameters of GA, HFO-1, and PSO Algorithms.

GA	HFO-1	PSO
Crossover probability, pc: 0.95 Mutation probability, pm: 0.001 Elitism rate, Er: 0.2	MF= 8 qo= 2 randWalk=true the number of workers: 15 the number of onlookers: 15	Inertia Weight: wMax: 0.9, wMin = 0.2 Cognitive and Social Coefficients: c1: 2, c2: 2

For all optimization algorithms: the size of population: 30, maximum number of iterations: 15,000, the search range: [-1, 4], the number of variables: 1–7, depending on the selected model.

When the trials with a dipping time of 10 h were examined, it is seen that the models with the lowest RMSE, χ^2 and MAE and highest EF were predominantly Modified Henderson and Pabis I and Modified Henderson and Pabis II. In addition, in the 50 Brix "G" experiment, the lowest RMSE, χ^2 and MAE and highest EF values was in the Haghi and Andiz model with 7.89E-04, 7.67E-07, 5.70E-04 and 1.00E+ 00, respectively. In 10-hour trials, the lowest RMSE, χ^2 and MAE and highest EF values was generally found in the Modified Henderson and Pabis I model with 5.74E-04, 4.43E-07, 4.08E-04 and 1.00E+ 00 in the 70 Brix "S" trial, respectively.

In the samples dried after 20 h of dipping, it was observed that the Modified Henderson and Pabis I and Modified Henderson and Pabis II models achieved the lowest RMSE, χ^2 and MAE and highest EF values. However, unlike the others, in the 70 Brix "G" value experiment, the Haghi and Andiz model is at the lowest level with a RMSE, χ^2 and MAE value of 1.74E-03, 3.89E-06 and 1.12E-03, respectively, and highest EF values with 1.00E+ 00. Among the experiments with 20 h of dipping time, the lowest RMSE, χ^2 and MAE and highest EF values was found in the 70 Brix "S" trial and the Modified Henderson and Pabis I model with a value of 7.48E-03, 3.89E-06, 1.11E-03 and 1.00E+ 00, respectively.

As a result of the drying trials carried out with 30 h of dipping time, the Modified Henderson and Pabis I and Modified Henderson and Pabis II models stood out with the lowest RMSE, χ^2 and MAE and highest EF values, as in the trials with 10 and 20 h of dipping time. Again, as in other dipping periods, a different result emerged in one trial. This difference was observed in the 50 Brix "S" experiment with a RMSE, χ^2, MAE and EF values value of 1.11E-03, 1.45E-06, 9.06E-04 and 1.00E+ 00, respectively, by Alibas et al. model was found. Among all the experiments with 30 h dipping period, the lowest RMSE, χ^2 and MAE and highest EF values value was seen in the Modified Henderson and Pabis I model in the 70 Brix "S" experiment with a value of 7.11E-04, 5.57E-07, 5.10E-04 and 1.00E+ 00, respectively. Additionally, in the 70 Brix "G" trial, the lowest RMSE, χ^2 and MAE and highest EF values, which were very close in both the Modified Henderson and Pabis I and Modified Henderson and Pabis II models.

When all dipping times were examined separately, it was determined that the lowest RMSE, χ^2 and MAE and highest EF values value was in the 70 Brix "S" trial and the Modified Henderson and Pabis I model. In

Table 3
Models giving the three lowest RMSE, χ^2 and MAE and highest EF values in trials with all algorithms.

Dipping Time	Pre-treatment	Model Names	HFO-1				GA				PSO			
			RMSE	χ^2	EF	MAE	RMSE	χ^2	EF	MAE	RMSE	χ^2	EF	MAE
10 h	S50	M. Henderson & Pabis II	1.05E−03	1.47E−06	1.00E+ 00	6.78E−04	4.28E−01	2.55E−01	−6.67E+ 00	4.10E−01	1.05E−03	1.47E−06	1.00E+ 00	6.67E−04
		Alibas et al.	1.19E−03	1.71E−06	1.00E+ 00	7.73E−04	1.99E−01	1.22E−02	5.92E−01	7.82E−02	1.19E−03	1.71E−06	1.00E+ 00	7.73E−04
		Haghi & Andiz	1.24E−03	2.07E−06	1.00E+ 00	7.67E−04	7.78E+ 01	7.97E+ 03	−2.53E+ 05	6.81E+ 01	2.60E−02	8.89E−04	9.72E−01	2.14E−02
	S60	M. Henderson & Pabis I	7.46E−04	4.55E−03	8.09E−01	3.54E−02	4.00E−01	2.10E−01	−7.80E+ 00	3.68E−01	3.39E−02	1.52E−03	9.36E−01	2.85E−02
		Haghi & Andiz	7.90E−04	7.79E−07	1.00E+ 00	6.21E−04	1.30E+ 01	2.34E+ 02	−9.80E+ 03	1.15E+ 01	1.30E−01	6.60E−04	9.72E−01	1.82E−02
		Alibas et al.	8.52E−04	9.34E−07	1.00E+ 00	7.07E−04	4.37E−02	2.38E−03	8.95E−01	3.45E−02	8.81E−04	1.00E−06	1.00E+ 00	7.29E−04
	S70	M. Henderson & Pabis I	5.74E−04	4.43E−07	1.00E+ 00	4.08E−04	2.76E−01	1.00E−01	−4.04E+ 00	2.42E−01	4.50E−03	2.64E−05	9.99E−01	3.10E−03
		Alibas et al.	7.06E−04	6.19E−07	1.00E+ 00	5.17E−04	7.03E−02	6.18E−03	6.73E−01	5.96E−02	7.06E−04	6.19E−07	1.00E+ 00	5.17E−04
		M. Henderson & Pabis II	7.17E−04	3.80E−03	8.19E−01	1.10E−02	3.61E−02	1.81E−03	9.14E−01	3.00E−02	1.16E−03	1.89E−06	1.00E+ 00	9.69E−04
	G50	Haghi & Andiz	7.89E−04	7.67E−07	1.00E+ 00	5.70E−04	3.60E+ 01	1.70E+ 03	−5.24E+ 04	3.14E+ 01	1.26E−02	1.25E−03	9.62E−01	2.50E−02
		M. Henderson & Pabis I	9.39E−04	1.06E−06	1.00E+ 00	7.02E−04	3.20E−01	1.35E−01	−3.16E+ 00	2.98E−01	2.76E−03	1.06E−06	1.00E+ 00	7.02E−04
		Alibas et al.	1.27E−03	1.84E−06	1.00E+ 00	1.00E−03	8.55E−02	9.13E−03	7.04E−01	7.10E−02	2.48E−03	1.84E−06	1.00E+ 00	1.00E−03
	G60	M. Henderson & Pabis I	8.75E−04	9.89E−07	1.00E+ 00	6.70E−04	6.82E−02	6.13E−03	7.63E−01	5.84E−02	8.92E−04	1.02E−06	1.00E+ 00	7.09E−04
		M. Henderson & Pabis II	8.76E−04	1.27E−06	1.00E+ 00	7.27E−04	4.97E−02	3.58E−01	−1.21E+ 01	2.63E−01	2.51E−03	9.43E−06	1.00E+ 00	2.28E−03
		Haghi & Andiz	1.04E−03	1.37E−06	1.00E+ 00	7.07E−04	3.41E+ 01	1.84E+ 03	−7.14E+ 04	3.34E+ 01	1.26E−02	6.49E+ 00	−2.50E+ 02	2.01E+ 00
	G70	M. Henderson & Pabis II	1.40E−03	2.60E−06	1.00E+ 00	9.18E−04	6.26E−02	5.44E−03	7.59E−01	5.45E−02	2.39E−03	7.61E−06	1.00E+ 00	2.06E−03
		M. Henderson & Pabis I	1.50E−03	2.72E−06	1.00E+ 00	8.96E−04	3.86E−01	1.97E−01	−8.18E+ 00	3.51E−01	4.32E−03	2.46E−05	9.99E−01	2.39E−03
		Haghi & Andiz	2.16E−03	5.92E−06	1.00E+ 00	1.30E−03	1.23E+ 02	2.00E+ 04	−9.34E+ 05	1.08E+ 02	3.20E−03	1.27E−05	9.99E−01	2.25E−03
20 h	S50	M. Henderson & Pabis II	1.32E−03	3.98E−05	9.98E−01	2.07E−03	3.52E−02	1.77E−03	9.31E−01	3.02E−02	2.20E−03	2.41E−03	9.06E−01	1.01E−02
		Haghi & Andiz	2.22E−03	6.95E−06	1.00E+ 00	1.45E−03	1.52E+ 01	3.03E+ 02	−1.24E+ 04	1.25E+ 01	2.53E−02	7.55E−01	−3.00E+ 01	1.73E−01
		M. Henderson & Pabis I	2.41E−03	7.91E−06	1.00E+ 00	1.54E−03	3.63E−01	1.73E−01	−6.10E+ 00	3.27E−01	5.32E−02	3.72E−03	8.47E−01	4.31E−02
	S60	M. Henderson & Pabis I	7.69E−04	5.82E−07	1.00E+ 00	4.68E−04	2.95E−01	1.14E−01	−3.64E+ 00	2.54E−01	3.52E−02	1.63E−03	9.34E−01	2.92E−02
		Haghi & Andiz	9.66E−04	1.07E−06	1.00E+ 00	6.74E−04	1.27E+ 02	2.12E+ 04	−8.61E+ 05	1.11E+ 02	5.40E−03	3.81E−05	9.98E−01	4.48E−03
		Alibas et al.	1.06E−03	1.29E−06	1.00E+ 00	8.09E−04	8.23E−02	8.47E−03	6.39E−01	6.62E−02	1.04E−01	1.36E−02	4.20E−01	7.78E−02
	S70	M. Henderson & Pabis I	7.48E−04	6.79E−07	1.00E+ 00	5.01E−04	2.38E−01	7.46E−02	−4.84E+ 00	2.01E−01	7.83E−04	7.00E−07	1.00E+ 00	5.25E−04
		Alibas et al.	9.65E−04	1.20E−06	1.00E+ 00	7.71E−04	6.15E−02	4.78E−03	6.06E−01	5.56E−02	9.65E−04	1.20E−06	1.00E+ 00	7.71E−04
		Haghi and Andiz	9.89E−04	1.38E−06	1.00E+ 00	6.53E−04	1.37E+ 01	2.46E+ 02	−1.93E+ 04	1.20E+ 01	5.92E−03	4.68E−05	9.96E−01	5.05E−03
	G50	M. Henderson & Pabis I	9.18E−04	1.08E−06	1.00E+ 00	6.08E−04	3.17E−01	1.32E−01	−3.77E+ 00	2.80E−01	2.39E−03	7.22E−06	1.00E+ 00	1.47E−03
		Haghi & Andiz	1.07E−03	1.55E−06	1.00E+ 00	8.26E−04	2.19E+ 01	6.31E+ 02	−2.28E+ 04	1.86E+ 01	2.59E−02	8.88E−04	9.68E−01	2.13E−02
		Alibas et al.	1.47E−03	2.58E−06	1.00E+ 00	1.17E−03	5.52E−02	3.80E−03	8.56E−01	4.79E−02	1.11E−01	1.53E−02	4.19E−01	8.27E−02
	G60	M. Henderson & Pabis II	1.09E−03	7.76E−06	1.00E+ 00	1.09E−03	7.17E−02	7.11E−03	7.57E−01	6.13E−02	3.03E−03	1.35E−05	1.00E+ 00	2.59E−03
		M. Henderson & Pabis I	1.87E−03	4.49E−06	1.00E+ 00	1.01E−03	8.50E−02	9.53E−03	6.57E−01	7.35E−02	5.62E−02	4.15E−03	8.50E−01	4.51E−02
		Haghi & Andiz	1.92E−03	4.61E−06	1.00E+ 00	1.04E−03	6.46E+ 01	3.47E+ 05	−1.25E+ 07	4.13E+ 02	2.97E−02	1.17E−03	9.58E−01	2.44E−02
	G70	Haghi & Andiz	1.74E−03	3.89E−06	1.00E+ 00	1.12E−03	4.39E+ 01	2.53E+ 03	−1.30E+ 05	3.68E+ 01	1.92E−02	4.93E−04	9.75E−01	1.59E−02
		M. Henderson & Pabis II	1.75E−03	3.79E−06	1.00E+ 00	8.93E−04	1.17E−01	1.89E−02	7.98E−02	9.67E−02	3.77E−03	3.20E−05	9.98E−01	3.72E−03
		M. Henderson & Pabis I	1.76E−03	5.61E−04	9.71E−01	1.78E−02	1.89E−01	4.72E−02	−1.43E+ 00	1.53E−01	1.76E−03	3.59E−06	1.00E+ 00	9.78E−04
30 h	S50	Alibas et al.	1.11E−03	1.45E−06	1.00E+ 00	9.06E−04	1.13E−01	1.59E−02	5.34E−01	9.34E−02	2.48E−03	7.68E−06	1.00E+ 00	1.74E−03
		M. Henderson & Pabis II	1.12E−03	1.63E−06	1.00E+ 00	9.02E−04	8.78E−02	1.07E−02	7.19E−01	6.60E−02	2.08E−02	*UC*	*UC*	*UC*
		M. Henderson & Pabis I	1.18E−03	1.74E−06	1.00E+ 00	9.47E−04	2.09E−01	5.73E−02	−5.91E−01	1.77E−01	1.33E−03	2.15E−06	1.00E+ 00	1.08E−03
	S60	M. Henderson & Pabis I	8.71E−04	9.20E−07	1.00E+ 00	6.62E−04	4.79E−01	3.02E−01	−1.06E+ 01	4.61E−01	1.56E−03	3.71E−06	1.00E+ 00	1.09E−03
		M. Henderson & Pabis II	9.30E−04	2.37E−05	9.99E−01	1.51E−03	1.09E−01	1.66E−02	3.96E−01	9.00E−02	2.34E−03	3.08E−05	9.99E−01	2.68E−03
		Haghi & Andiz	1.24E−03	4.88E−03	8.12E−01	5.91E−02	2.99E+ 01	1.17E+ 03	−4.52E+ 04	2.61E+ 01	2.43E−02	7.79E−04	9.70E−01	1.99E−02
	S70	M. Henderson & Pabis I	7.11E−04	5.57E−07	1.00E+ 00	5.10E−04	1.40E−01	2.56E−02	−3.52E−01	1.18E−01	7.11E−04	5.57E−07	1.00E+ 00	5.10E−04
		M. Henderson & Pabis II	7.61E−04	8.50E−07	1.00E+ 00	6.48E−04	7.47E−02	7.74E−03	6.12E−01	6.41E−02	7.11E−04	5.88E−07	1.00E+ 00	5.10E−04
		Haghi & Andiz	9.08E−04	1.02E−06	1.00E+ 00	6.74E−04	2.09E+ 02	5.74E+ 04	−3.03E+ 06	1.81E+ 02	2.02E−02	5.39E−04	9.72E−01	1.67E−02
	G50	M. Henderson & Pabis II	8.38E−04	3.05E−05	9.99E−01	1.52E−03	9.49E−02	1.25E−02	6.33E−01	7.93E−02	2.01E−02	5.65E−04	9.83E−01	1.73E−02
		M. Henderson & Pabis I	9.85E−04	1.25E−06	1.00E+ 00	6.69E−04	1.73E−01	3.94E−02	−2.22E−01	1.44E−01	7.12E−02	6.67E−03	7.93E−01	6.03E−02
		Haghi & Andiz	1.12E−03	1.61E−06	1.00E+ 00	7.79E−04	3.16E+ 01	1.32E+ 03	−4.09E+ 04	2.76E+ 01	2.46E−03	7.73E−06	1.00E+ 00	1.85E−03
	G60	M. Henderson & Pabis I	1.19E−03	2.08E−06	1.00E+ 00	7.93E−04	1.08E−01	1.54E−02	3.48E−01	9.40E−02	5.23E−02	3.60E−03	8.48E−01	4.19E−02
		M. Henderson & Pabis II	1.20E−03	2.29E−06	1.00E+ 00	8.74E−04	3.70E−01	1.90E−01	−6.61E+ 00	3.31E−01	1.22E−03	2.31E−06	1.00E+ 00	9.43E−04
		Haghi & Andiz	1.43E−03	2.86E−06	1.00E+ 00	9.31E−04	1.40E+ 02	2.57E+ 04	−1.09E+ 06	1.22E+ 02	2.55E−02	8.60E−04	9.64E−01	2.14E−02
	G70	M. Henderson & Pabis I	7.86E−04	8.45E−07	1.00E+ 00	5.38E−04	3.47E−01	1.58E−01	−7.74E+ 00	3.03E−01	4.47E−02	2.62E−03	8.55E−01	3.57E−02
		M. Henderson & Pabis II	7.86E−04	9.31E−07	1.00E+ 00	5.78E−04	4.85E−02	3.32E−03	8.27E−01	3.74E−02	3.03E−02	1.27E−03	9.34E−01	2.47E−02
		Haghi & Andiz	8.61E−04	1.07E−06	1.00E+ 00	6.36E−04	4.67E+ 01	3.03E+ 03	−1.67E+ 05	4.20E+ 01	1.22E−02	1.94E−04	9.89E−01	1.00E−02
NP		M. Henderson & Pabis II	1.96E−03	5.31E−06	1.00E+ 00	1.32E−03	1.23E−01	2.11E−02	8.11E−01	1.03E−01	1.19E−02	1.98E−04	9.98E−01	9.82E−03
		Alibas et al.	3.88E−03	1.82E−05	1.00E+ 00	2.92E−03	1.74E−01	3.98E−02	6.05E−01	1.57E−01	6.49E−03	5.21E−05	9.99E−01	4.29E−03
		Haghi & Andiz	4.67E−03	2.81E−05	1.00E+ 00	3.21E−03	9.66E−02	1.23E−02	8.84E−01	7.81E−02	2.70E−02	9.58E−04	9.91E−01	2.39E−02

UC: Uncertain, NP: Non pre-treatment

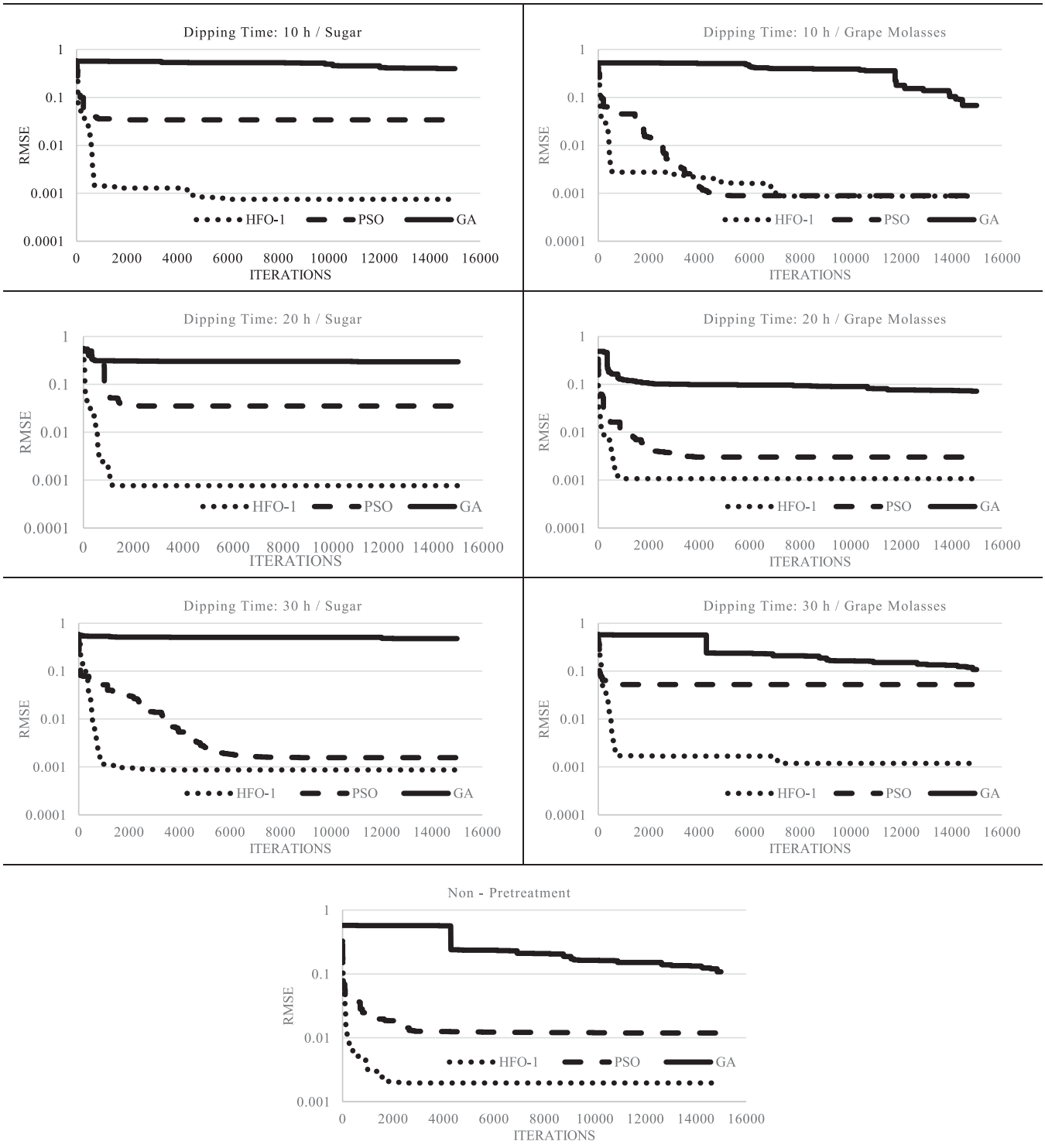

Fig. 1. RMSE performance for examined algorithms at 60 Brix.

samples non-pretreatment "NP", the lowest RMSE, χ^2 and MAE and highest EF values were found in the Modified Henderson and Pabis II model with 1.96E-03, 5.31E-06, 1.32E-03 and 1.00E+ 00, respectively. Models at the 10-hour experiments, the first three lowest RMSE, χ^2 and MAE and highest EF values are generally Modified Henderson and Pabis I, Modified Henderson and Pabis II, Alibas et al. and Haghi and Andiz models. The same situation is observed in the 20 and 30 h dipping period trials and the "NP" trial. Although there are four models that give the best results, it has been determined that the best models among them are the Modified Henderson and Pabis I and Modified Henderson and Pabis II models.

In addition to the tables, the distribution of experimental and predicted moisture ratio values were given in Fig. 2 for the best models. The data points are banded around a 45 degrees straight line, demonstrating the suitability of the model in describing the thin-layer drying behavior of the fresh bitter gourd samples.

In addition to the above studies, the robustness test of the models was also performed. Noise was generated using a Normal Gaussian

Table 4
Models coefficients of HFO-1 algorithm with the lowest RMSE to the samples.

Dipping Time	Pre-treatment	Model Names	Model Constants										RMSE	χ^2	EF	MAE
			a	k	n	b	g	c	h	d	e	f				
10 h	S50	M. Hen. & P. II	4.39E−01	3.10E+ 00	−1.00E+ 00	6.51E−01	1.54E−02	3.49E−01	1.63E−01				1.05E−03	1.47E−06	1.00E+ 00	6.78E−04
	S60	M. Hen. & P. I	4.97E−01	5.24E−05		4.75E−01	1.47E−02	2.76E−02	5.15E−02				7.46E−04	4.55E−03	8.09E−01	3.54E−02
	S70	M. Hen. & P. I	5.25E−01	4.60E−05		4.24E−01	1.42E−02	5.02E−02	1.45E−01				5.74E−04	4.43E−07	1.00E+ 00	4.08E−04
	G50	Haghi & Andiz	7.43E−01			2.13E−02		9.18E−01		−1.11E−06	7.32E−04	2.56E−01	7.89E−04	7.67E−07	1.00E+ 00	5.70E−04
	G60	M. Hen. & P. I	4.95E−01	1.76E−02		2.95E−02	1.86E−01	4.76E−01	1.80E−04				8.75E−04	9.89E−07	1.00E+ 00	6.70E−04
	G70	M. Hen. & P. II	5.06E−01	1.28E−11	3.63E+ 00	4.52E−01	1.52E−02	4.19E−02	3.88E+ 00				1.40E−03	2.60E−06	1.00E+ 00	9.18E−04
20 h	S50	M. Hen. & P. II	7.64E−01	3.37E−01	5.50E−02	−2.46E−01	1.48E−01	5.08E−01	1.82E−02				1.32E−03	3.98E−05	9.98E−01	2.07E−03
	S60	M. Hen. & P. I	4.99E−01	1.66E−02		2.09E−02	3.89E+ 00	4.80E−01	7.08E−05				7.69E−04	5.82E−07	1.00E+ 00	4.68E−04
	S70	M. Hen. & P. I	6.24E−01	1.01E−04		5.05E−02	1.97E−01	3.25E−01	1.56E−02				7.48E−04	6.79E−07	1.00E+ 00	5.01E−04
	G50	M. Hen. & P. I	5.16E−01	1.70E−02		2.21E−02	2.69E+ 00	4.62E−01	1.81E−04				9.18E−04	1.08E−06	1.00E+ 00	6.08E−04
	G60	M. Hen. & P. II	9.15E−01	4.49E−01	8.82E−02	4.97E−01	2.08E−02	−4.01E−01	1.89E−01				1.09E−03	7.76E−06	1.00E+ 00	1.09E−03
	G70	Haghi & Andiz	4.03E−01			1.90E−02		1.01E+ 00		2.86E−07	−3.00E−04	5.97E−01	1.74E−03	3.89E−06	1.00E+ 00	1.12E−03
30 h	S50	Alibas et al.	5.89E−01	−4.32E−02	2.56E−01	−1.54E−02	4.11E−01						1.11E−03	1.45E−06	1.00E+ 00	9.06E−04
	S60	M. Hen. & P. I	5.22E−01	1.56E−02		−2.12E−02	4.00E+ 00	5.00E−01	1.02E−04				8.71E−04	9.20E−07	1.00E+ 00	6.62E−04
	S70	M. Hen. & P. I	4.37E−01	1.55E−02		5.76E−01	1.08E−04	−1.33E−02	3.88E+ 00				7.11E−04	5.57E−07	1.00E+ 00	5.10E−04
	G50	M. Hen. & P. II	1.51E+ 00	1.07E+ 00	3.03E−02	5.58E−01	1.65E−02	−6.72E−01	2.63E−01				8.38E−04	3.05E−05	9.99E−01	1.52E−03
	G60	M. Hen. & P. I	5.00E−01	1.75E−02		−1.92E−02	4.00E+ 00	5.19E−01	1.36E−04				1.19E−03	2.08E−06	1.00E+ 00	7.93E−04
	G70	M. Hen. & P. I	5.89E−01	1.68E−04		4.20E−01	1.73E−02	−9.48E−03	2.99E−01				7.86E−04	8.45E−07	1.00E+ 00	5.38E−04
		M. Hen. & P. II	6.57E−02	7.02E−02	−2.87E−02	4.20E−01	1.73E−02	5.27E−01	1.89E−04				7.86E−04	9.31E−07	1.00E+ 00	5.78E−04
NP		M. Hen. & P. II	1.05E−01	9.00E−01	2.82E−14	1.90E+ 00	1.70E−02	−1.00E+ 00	3.05E−02				1.96E−03	5.31E−06	1.00E+ 00	1.32E−03

distribution with a standard deviation of 0.5 centered on the input values. All models were given the same Gaussian noise distribution. Since the best results obtained with HFO-1 and samples dipped in 70 Brix sugar for 10 h, the robustness test was performed for this trial. The best models for the noiseless input value are Modified Henderson Pabis I, Alibas et al., Modified Henderson Pabis II, and Haghi and Andiz, respectively. The best models for the noisy input values are Haghi and Andiz, Alibaş et al., and Midilli et al., respectively. Changes in the models are shown with the ratio of percentage change. Negative values indicate improvement. More clearly, it indicates that the RMSE value calculated with noisy data is smaller than the RMSE value calculated with noiseless data. This may seem confusing at first because noise is normally expected to increase the error rate. However, there may be several possible reasons for this, including: random improvement, overfitting, data set characteristics, or noise type. Positive values indicate the deterioration in the models and are the expected situation. Values close to 0 in this ratio are evidence of the robustness of the models against noise. According to the data in the table, the most robust models are the models with the least difference between the "RMSE_noisy" and "RMSE" values. According to these criteria: It shows that Henderson and Pabis is very little or almost not affected by noise. This highlights the model as the most robust. In general, it can be said that unsuccessful models are more robust to noise. Newton and Midilli et al. models also showed very low sensitivity to noise, that is, there are very small differences between RMSE values. These models can also be considered very robust. In contrast, “Demir et al.” and “Modified Henderson and Pabis I”, “Modified Henderson and Pabis II” and “Midilli and Kucuk” models showed huge increases in RMSE values when noise was added. On the other hand, the "Modified Henderson and Pabis I", "Modified Henderson and Pabis II" and "Midilli and Kucuk" models showed huge increases in RMSE values when noise was added. These models are the weakest and least robust models against noise. The coefficients of these models are very sensitive to noise and the results obtained with noisy data are far from reliable. As a result, the models of Henderson and Pabis, Newton and Midilli et al. show the highest robustness to noisy data. These models tend to produce results that are more resistant to random variations in the data set or measurement errors (Table 5).

In solution of these different models with non-linear analysis by different computer softwares, Levenberg-Marquardt back propagation algorithm is generally used (Da Silva et al., 2014; Tepe, 2023b; Maamar et al., 2023). The proposed genetic algorithms (GA) approach was employed to determine the parameters of the modified Page model in regression routines applied for all experimental runs (Erenturk and Erenturk, 2007). So, these data could be used to optimize drying time in industry practically. Engineers can determine how long a specific product needs to dry to reach final moisture content, by avoiding under or over-drying. In addition, drying methods or conditions could be compared specifically. Some of the design parameters could be determined by using MR. Monitoring MR values in real time, the process could be controlled to reach the final moisture content with high quality.

Shelf life is generally determined by moisture content and water activity (a_w). Thin-layer drying models are also used to estimate how quickly and to what extent a product will lose moisture under specific conditions. Using the relationship between these models and sorption isotherms (moisture content and water activity), microbial growth can be assessed by determining the time required to reach the critical moisture content and water activity after drying. The design of the dryer can be realized by finding the required drying time using the relationship between the coefficients in the thin layer drying models and the drying conditions. Sheet drying models can also be used for energy efficiency because they allow you to accurately predict how much drying time and heat are actually needed, preventing overheating, overdrying, or running the dryer for longer than necessary. If the estimated moisture content values are correct, the results obtained from them will also be more accurate.

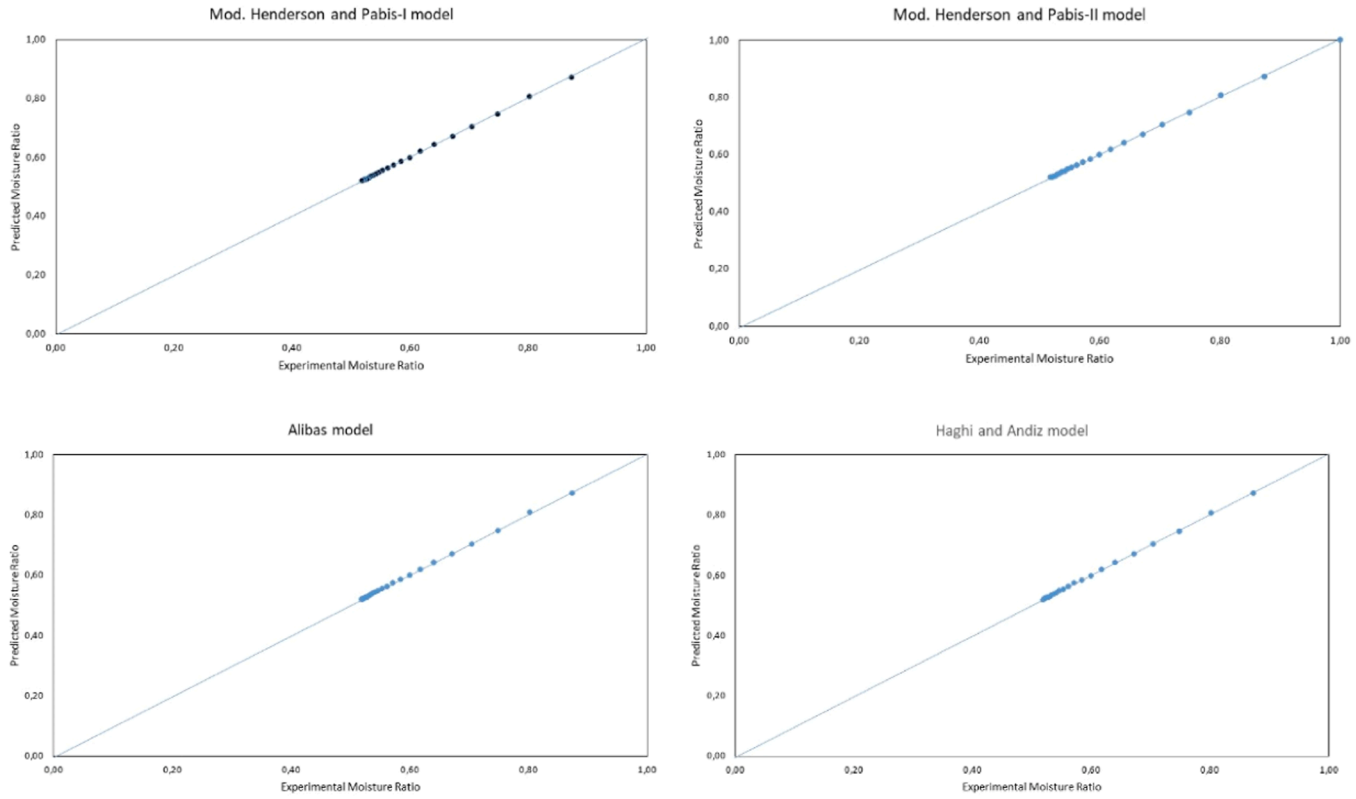

Fig. 2. Experimental and predicted moisture ratio values for best models for samples dipped in 70 Brix sugar for 10 h.

Table 5
Robustness analysis of models for the case with dipped in 70 Brix sugar for 10 h.

Model	RMSE_with_noise	RMSE	Ratio of percentage change
Newton	9,79E−02	9,81E−02	−0,17 %
Henderson and Pabis	5,96E−02	5,96E−02	−0,04 %
Page	2,49E−02	2,35E−02	5,76 %
Two-term	4,63E−03	4,50E−03	2,84 %
Modified Henderson and Pabis I	3,46E−01	5,74E−04	60140,07 %
Modified Henderson and Pabis II	3,19E−01	7,17E−04	44344,30 %
Midilli et al.	4,28E−03	4,30E−03	−0,45 %
Verma et al.	4,96E−03	5,14E−03	−3,45 %
Demir et al.	3.47E+ 01	1.68E−03	2063939.48 %
Alibas et al.	1,60E−03	7,06E−04	126,22 %
Haghi and Andiz	1,49E−03	7,17E−04	107,64 %
Midilli and Kucuk	1,05E+ 00	2,31E−02	4447,78 %
Yun et al.	1,84E−01	1,23E−01	49,65 %
Hii et al.	8,98E−03	1,48E−02	−39,30 %

4. Conclusions

In this paper, the metaheuristic optimization algorithm (HFO-1), genetic algorithm (GA) and particle swarm optimization algorithm (PSO) are comparatively studied in the context of parameter optimization of drying models where HFO-1 algorithm is first time used in the literature. The 14 common thin layer drying models, considered in the paper, are first time collectively used for drying bitter gourd fruit. Moreover, to demonstrate the practical relevance of the study, robustness tests were conducted on the best-performing models using HFO-1. The motivation of using HFO-1 is its ability to have both the success and fast convergence better than GA and PSO, particularly in low dimensional search space. It uses random walk behavior and updates multiple dimensions of the solution at once.

The evaluation showed that the Modified Henderson and Pabis I and II models generally produced the lowest RMSE, χ^2, and MAE values and the highest EF values. In specific trials, the Haghi and Andiz and Alibas et al. models also performed best. Among the top three models, Modified Henderson and Pabis I and II appeared most frequently. With respect to RMSE, HFO-1 outperformed PSO and GA by at least 6.84E+ 02 % for samples dipped in 70 Brix sugar for 10 h. Robustness analysis indicated that the Henderson and Pabis model was highly resistant to noisy data. Overall, considering both optimization and robustness, the Midilli et al. model was identified as the most suitable.

The manuscript demonstrates how the models can be applied to optimize industrial drying time, support process control and quality monitoring, predict shelf life through the relationship between moisture content and water activity, guide the design of more efficient dryers, and improve energy efficiency by preventing over-drying. The results indicate that MR values can be predicted with lower errors, and the HFO-1 algorithm outperforms commonly used methods such as the Genetic Algorithm and Particle Swarm Optimization. This suggests that HFO-1 could be practically integrated into different software applications. Moreover, by employing advanced algorithms and computer-based tools, thin-layer drying models can be further developed, enabling highly accurate representations of the drying process and reliable predictions based on values closely aligned with experimental results.

Despite the promising results, this study has some limitations. The findings are specific to bitter gourd under the pretreatment and drying conditions tested. Therefore, future research should focus on validating the performance of HFO-1 across a wider range of fruits and vegetables with different characteristics. Furthermore, exploring the hybridization of HFO-1 with other algorithms or local search techniques could potentially provide even more powerful and efficient optimization tools. Finally, applying these optimized models to a real-time industrial control system will be the ultimate test of their practical utility.

CRediT authorship contribution statement

ERTEKIN CAN: Writing – review & editing, Writing – original draft, Supervision, Resources, Project administration, Methodology, Investigation, Formal analysis, Data curation, Conceptualization. **Uğur Ercan:** Writing – review & editing, Writing – original draft, Visualization, Software, Methodology, Formal analysis. **Boyar İsmail:** Writing – review & editing, Writing – original draft, Validation, Resources, Methodology, Formal analysis, Data curation. **Tugce Ozsan Kilic:** Writing – review & editing, Writing – original draft, Validation, Resources, Data curation, Conceptualization. **Zeki Yetgin:** Writing – review & editing, Writing – original draft, Visualization, Software, Methodology, Formal analysis.

References

Abualigah, L., Elaziz, M.A., Khasawneh, A.M., Alshinwan, M., Ibrahim, R.A., Al-Qaness, M.A., Mirjalili, S., Sumari, P., Gandomi, A.H., 2022. Meta-heuristic optimization algorithms for solving real-world mechanical engineering design problems: a comprehensive survey, applications, comparative analysis, and results. Neural Comput. Appl. 1–30.

Ahmed, M., Faisal, M., Laskar, A., Abdullah, A., Shahadat, M., Umar, K., Kamyab, H., Ubaidullah, M., Panditj, B., Prakash, C., Yusuf, M., 2023. Experimental studies for thin layer model validation and microwave drying characteristics of beetroot considering energy optimization. Fuel 346, 128345.

Akman, H.E., Boyar, I., Gozlekci, S., Saracoglu, O., Ertekin, C., 2022. Effects of convective drying of quince fruit (*Cydonia oblonga*) on color, antioxidant activity and phenolic compounds under various fruit juice dipping pre-treatments. Agriculture 12, 1224.

Alibas, I., 2012. Selection of a the best suitable thin-layer drying mathematical model for vacuum dried red chili pepper. J. Biol. Environ. Sci. 6, 17.

Alvarez-Suarez, J.M., Giampieri, F., Tulipani, S., Casoli, T., Di Stefano, G., Gonzalez-Paramas, A.M., Santos-Buelga, C., Busco, F., Quiles, J.L., Cordero, M.D., Bompadre, S., Mezzetti, B., Battino, M., 2014. One month strawberry-rich anthocyanin supplementation ameliorates cardiovascular risk, oxidative stress markers and platelet activation in humans. J. Nutr. Biochem 25, 289–294.

Ambawat, S., Sharma, A., Saini, R.K., 2022. Mathematical modeling of thin layer drying kinetics and moisture diffusivity study of pretreated moringa pleifera leaves using fluidized bed dryer. Process 10, 2464.

Ardabili, G.A., Godini, N., Salehi, F., 2023. Selection and evaluation of thin layer drying models for describing drying kinetics of garlic slices in an infrared dryer. Iran. J. Food Sci. Ind. 19, 377–385.

Argo, B.D., Sandra, S., Ubaidillah, U., 2018. Mathematical modeling on the thin layer drying kinetics of cassava chips in a multipurpose convective-type tray dryer heated by a gas burner. J. Mech. Sci. Technol. 32, 3427–3435.

Arslan, D., Ozcan, M.M., 2012. Evaluation of drying methods with respect to drying kinetics, mineral content, and color characteristics of savory leaves. Food Bioprocess Technol. 5, 983–991.

Balbay, A., Sahin, O., 2012. Microwave drying kinetics of a Thin-Layer liquorice root. Dry. Technol. 30, 859–864. https://doi.org/10.1080/07373937.2012.670682.

Bchir, B., Besbes, S., Karoui, R., Paquot, M., Attia, H., Blecker, C., 2012. Osmotic dehydration kinetics of pomegranate seeds using date juice as an immersion solution base. Food Bioprocess Tech. 5, 999–1009. https://doi.org/10.1007/s11947-010-0442-1.

Cai, Z.L., Ma, X.Q., Qing, X., Yu, Z.S., 2015. Drying kinetics and characteristics of sewage sludge/rice straw mixture. Dry. Technol. 33, 1500–1509. https://doi.org/10.1080/07373937.2015.1021928.

Corzo, O., Bracho, N., Alvarez, C., 2011. Determination of suitable thin layer model for air drying of mango slices (*Mangifera indica* L.) at different air temperatures and velocities. J. Food Process Eng. 34, 332–350.

Da Silva, W.P., E Silva, C.M.D.P.S., Gama, F.J.A., Gomes, J.P., 2014. Mathematical models to describe thin-layer drying and to determine drying rate of whole bananas. King Saud. Univ. J. Saudi Soc. Agric. Sci. 13, 67–74.

Delgado, T., Pereira, J.A., Baptista, P., Casal, S., Ramalhosa, E., 2014. Shell's influence on drying kinetics, color and volumetric shrinkage of Castanea sativa mill. Fruits. Food Res. Int. 55, 426–435.

Demir, V., Gunhan, T., Yagcioglu, A.K., 2007. Mathematical modelling of convection drying of green table olives. Biosyst. Eng. 98, 47–53.

Doymaz, I., 2009. An experimental study on drying of Green apples. Dry. Technol. 27, 478–485. https://doi.org/10.1080/07373930802686065.

Erenturk, S., Erenturk, K., 2007. Comparison of genetic algorithm and neural network approaches for the drying process of carrot. J. Food Eng. 78, 905–912.

Erol, N.T., 2022. Mathematical modeling of thin layer dried potato and effects of different variables on drying behavior and quality characteristics. Potato Res. 65, 65–82.

Ertekin, C., Firat, M.Z., 2017. A comprehensive review of thin-layer drying models used in agricultural products. Crit. Rev. Food Sci. Nutr. 57, 701–717.

Ertekin, C., Heybeli, N., 2014. Thin-layer infrared drying of mint leaves. J. Food Process. Preserv. 38, 1480–1490.

Ghimire, A., Basnet, S., Poudel, R., 2020. Mathematical modeling of thin layer microwave drying of Jaya fish. Food Sci. Technol. Int. 27, 508–516.

Giampieri, F., Alvarez-Suarez, J.M., Battino, M., 2014. Strawberry and human health: effects beyond antioxidant activity. J. Agric. Food Chem. 62, 3867–3876.

Guo, H.L., Chen, Y., Xu, W., Xu, M.T., Sun, Y., Wang, X.C., Wang, X.Y., Luo, J., Zhang, H., Xiong, Y.K., 2022. Assessment of drying kinetics, textural and aroma attributes of mentha haplocalyx leaves during the hot air thin-layer drying process. Foods 11, 784. https://doi.org/10.3390/foods11060784.

Haghi, A.K., Angiz, F.Z., 2007. Heat and mass transfer in thermal dry-ing of wool: a theoretical approach. In: The Proceedings of the 5th Asia-Pasific Drying Conference, 1, pp. 443–448.

Hamdani, N., Sayyad, M., Olodegaragoze, A., 2006. Mathematical modeling of thin layer drying kinetics of apple slices. JUFoST 20060324. https://doi.org/10.1051/JUFFoST.

Hamrouni-Sellami, I., Wannes, W.A., Bettaieb, I., Berrima, S., Chahed, T., Marzouk, B., Limam, F., 2011. Qualitative and quantitative changes in the essential oil of *Laurus nobilis* L. Leaves as affected by different drying methods. Food Chem. 126, 691–697. https://doi.org/10.1016/j.foodchem.2010.11.022.

Hazar, D., Boyar, I., Dincer, C., Ertekin, C., 2023. Investigation of color and bioactive compounds of different colors from pansy (*Viola× wittrockiana gams.*) dried in hot air dryer. Horticulturae 9, 186.

Hii, C.L., Law, C.L., Cloke, M., 2009. Modeling using a new thin layer drying model and product quality of cocoa. J. Food Eng. 90, 191–198.

Hossain, M.A., Dey, P., Joy, R.I., 2021. Effect of osmotic pretreatment and drying temperature on drying kinetics, antioxidant activity, and overall quality of taikor (*Garcinia pedunculata* Roxb.) slices. Saudi J. Biol. Sci. 28, 7269–7280.

Hssaini, L., Ouaabou, R., Hanine, H., Razouk, R., Idlimam, A., 2021. Kinetics, energy efficiency and mathematical modeling of thin layer solar drying of figs (*Ficus carica* L.). Sci. Rep. 11, 21266. https://doi.org/10.1038/s41598-021-00690-z.

Jayashree, E., Zachariah, T.J., 2022. Modeling for thin layer drying of black pepper in a reverse air flow dryer. J. Food Process Eng. 46, e14202.

Jia, H., Rao, H., Wen, C., Mirjalili, S., 2023. Crayfish optimization algorithm. Artif. Intell. Rev. 56, 1919–1979.

Jin, W., Zhang, M., Shi, W., 2019. Evaluation of ultrasound pretreatment and drying methods on selected quality attributes of bitter melon (*Momordica charantia* L. Dry. Tech. 37, 387–396. https://doi.org/10.1080/07373937.2018.1458735.

Kamal, M.S., Shakil, M., Akter, T., Yasmin, S., Saeid, A., Khandaker, M.U., 2023. Moisture sorption behavior and effects of temperature, slice thickness and loading density on drying kinetics of a local sweet potato cultivar grown in Bangladesh. J. Food Process. Preserv., 5523400 (Article ID.).

Karaaslan, S., Ekinci, K., Ertekin, C., Kumbul, B.S., 2021. Thin layer peach drying in solar tunnel drier. ErwerbsObstbau 63, 65–73.

Karimi-Mamaghan, M., Mohammadi, M., Meyer, P., Karimi-Mamaghan, A.M., Talbi, E. G., 2022. Machine learning at the service of meta-heuristics for solving combinatorial optimization problems: a state-of-the-art. Eur. J. Oper. Res. 296, 393–422.

Kayisoglu, S., Ertekin, C., 2011. Vacuum drying kinetics of Barbunya bean. Philipp. Agric. Sci. 94 (2011), 285–291.

Kudri, S., Harshitha, T., Hegde, P., Tadkod, M., Deasei, S., Hemalatha, S., 2022. Effect of molasses, honey, and sugar on osmotic dehydration of muskmelon (*Cucumis melo* L.). Pharma Innov. 11, 162–166.

Kumar, K.S., Bhowmik, D., 2010. Traditional medicinal uses and therapeutic benefits of Momordica charantia linn. Int. J. Pharm. Sci. Rev. Res. 4, 23–28.

Lewicki, P.P., Lenart, A., 2006. Osmotic dehydration of fruits and vegetables. In: Mujumdar, A.S. (Ed.), Handbook of Industrial Drying, third ed. CRC Press. Taylor & Francis Group, LLC.

Maamar, M.I., Badraoui, M., Mazaizi, M., Mouakkir, L., 2023. Mathematical modeling on vacuum drying of olive pamace. Trends Sci. 20, 3822.

Mehta, D., Prasad, P., Bansal, V., Siddiqui, M.W., Sharma, A., 2017. Effect of drying techniques and treatment with blanching on the physicochemical analysis of bitter-gourd and capsicum. LWT 84, 479–488.

Midilli, A., Kucuk, H., 2023. Development of a new curve equation representing thin layer drying process. Energy Sources Part A Recovery Util. Environ. Eff. 45, 9717–9730.

Midilli, A., Kucuk, H., Yapar, Z., 2002. A new model for single-layer drying. Dry. Technol. 20, 1503–1513.

Mirjalili, S., 2024a. A simple implementation of Particle Swarm Optimization (PSO) Algorithm (⟨https://www.mathworks.com/matlabcentral/fileexchange/67429-a-simple-implementation-of-particle-swarm-optimization-pso-algorithm⟩), MATLAB Central File Exchange. Retrieved April 16, 2024.

Mirjalili, S., 2024b. The Continuous Version of The Genetic Algorithm (⟨https://www.mathworks.com/matlabcentral/fileexchange/67694-the-continuous-version-of-the-genetic-algorithm⟩), MATLAB Central File Exchange. Retrieved April 16, 2024.

Nguyen, L.T., Ha, N.M., Le, H.S.N., 2023a. Thin-Layer drying of burdock root in a convective dryer: drying kinetics and numerical simulation. J. Adv. Res. Fluid Mech. Therm. Sci. 104, 21–36.

Nguyen, T.T., Rosselo, C., Ratti, C., 2023b. Simple mathematical modeling to represent air drying kinetics of potato peel. J. Food Eng. 357, 111634.

Ozsan Kilic, T., Boyar, I., Dincer, C., Ertekin, C., Onus, A.N., 2023a. Effects of different osmotic Pre-Treatments on the drying characteristics, modeling and physicochemical properties of momordica charantia L. Slices. Agriculture 13, 1887.

Ozsan Kilic, T., Boyar, I., Gungor, K.K., Torun, M., Perendeci, N.A., Ertekin, C., Onus, A. N., 2023b. Improvement of hot air dried bitter gourd (*Momordica charantia* L.) product quality: optimization of drying and blanching process by experimental design. Agriculture 13, 1849.

Parisotto, E.I.B., Telekon, J.J., Laurindo, J.B., Carciofi, B.A.M., 2020. Mathematical modelling and experimental assessment of the cast-tape drying. Dry. Technol. 38, 1024–1035.

Polat, A., Izli, N., 2022. Determination of drying kinetics and quality parameters for drying apricot cubes with electrohydrodynamic, hot air and combined electrohydrodynamic-hot air drying methods. Dry. Technol. 40, 527–542. https://doi.org/10.1080/07373937.2020.1812633.

Rajkumar, G., Shanmugam, S., Galvao, M.D.S., Neta, M.T.S.L., Sandes, R.D.D., Mujumdar, A.S., Narain, N., 2017. Comparative evaluation of physical properties and aroma profile of carrot slices subjected to hot air and freeze drying. Dry. Technol. 35, 699–708. https://doi.org/10.1080/07373937.2016.1206925.

Roy, M., Bulbul, M.A.I., Hossain, M.A., Shourove, J.H., Ahmed, S., Sarkar, A., Biswas, R., Hossain, M.S., 2022. Study on the drying kinetics and quality parameters of osmotic pre-treated dried satkara (*Citrus macroptera*) fruits. J. Food Meas. Charact. 16, 471–485. https://doi.org/10.1007/s11694-021-01177-1.

Shahhoseini, R., Ghorbani, H., Karimi, S.R., Estaji, A., Moghaddam, M., 2013. Qualitative and quantitative changes in the essential oil of lemon verbena (*Lippia citriodora*) as affected by drying condition. Dry. Technol. 31, 1020–1028. https://doi.org/10.1080/07373937.2013.771649.

Sharma, P.R., Varma, A.J., 2014. Thermal stability of cellulose and their nanoparticles: effect of incremental increases in carboxyl and aldehyde groups. Carbohydr. Polym. 114, 339–343. https://doi.org/10.1013/j.carbpol.2014.08.032.

Singh, D., Sengar, M., Patel, S.K., Kumar, D., Pal, D., Giri, B.S., Singh, D., 2023. Drying characteristics of thin layer of potato (*Solanum tuberosum*): experimental and computational studies. Environ. Sci. Pollut. Res. https://doi.org/10.1007/s11356-022-25121-y.

Stanner, S.A., Hughes, J., Kelly, C.N.M., Buttriss, J., 2004. A review of the epidemiological evidence for the 'antioxidant hypothesis. Public Health Nutr. 7, 407–422.

Taheri-Garavand, A., Rafiee, S., Keyhani, A.R., 2011. Mathematical modeling of thin layer drying kinetics of tomato influence of air dryer conditions. Int. Trans. J. Eng. Manag. Appl. Sci. Technol. 2, 147–160.

Tepe, T.K., 2023a. Convective drying of potato slices: impact of ethanol pretreatment and time on drying behavior, comparison of thin-layer and artifcial neural network modeling, color properties, shrinkage ratio, and chemical and ATR-FTIR analysis of quality parameters. Potato Res. https://doi.org/10.1007/s11540-023-09663-3.

Tepe, T.K., 2023b. Enhancement of convective banana drying: effect of ethanol pretreatment on drying characteristics, color properties, shrinkage ratio and comparison of articial neural network and thin layer modeling. Karadeniz Fen. Bilim. Derg. 13, 1738–1758.

Turan, O.Y., Firatligil, F.E., 2019. Modeling and characteristics of thin layer convective air drying of thyme leaves. Czech J. Food Sci. 37, 128–134.

Wen, C., Jia, H., Wu, D., Rao, H., Li, S., Liu, Q., Abualigah, L., 2022. Modified remora optimization algorithm with multi strategies for global optimization problem. Mathematics 10, 3604.

Xia, J., Li, S., Huang, J., Yang, Z., Jaimoukha, I.M., Gunduz, D., 2023. Metalearning-Based alternating minimization algorithm for nonconvex optimization. IEEE Trans. Neural Netw. Learn. Syst. 34 (9), 5366–5380.

Yadav, A.K., Singh, S.V., 2014. Osmotic dehydration of fruits and vegetables: a review. J. Food Sci. Tech. 51, 1654–1673. https://doi.org/10.1007/s13197-012-0659-2.

Yaldiz, O., Ertekin, C., 2001. Thin layer solar drying of some vegetables. Dry. Technol. 19, 583–597.

Yan, J.K., Wu, L.X., Qiao, Z.R., Cai, W.D., Ma, H., 2019. Effect of different drying methods on the product quality and bioactive polysaccharides of bitter gourd (*Momordica charantia* L.) slices. Food Chem. 271, 588–596. https://doi.org/10.1016/j.foodchem.2018.08.012.

Yang, X., Wang, R., Zhao, D., Yu, F., Huang, C., Heidari, A.A., Cai, Z., Bourouis, S., Algarni, A.D., Chen, H., 2023. An adaptive quadratic interpolation and rounding mechanism sine cosine algorithm with application to constrained engineering optimization problems. Expert Syst. Appl. 213, 119041.

Yetgin, Z., Abaci, H., 2021. Honey formation optimization framework for design problems. Appl. Math. Comput. 394, 125815.

Yetgin, Z., Ercan, U., 2023. Honey formation optimization with single component for numerical function optimization: HFO-1. Neural Comput. Appl. 35, 24897–24923.

Yetgin, Z., Samdan, M., 2021. Honey formation optimization: HFO. Turk. J. Eng. 5, 81–88.

Yi, X.K., Wu, W.F., Zhang, Y.Q., Li, J.X., Luo, H.P., 2012. Thin layer drying characteristics and modeling of chineese jujubes. Math. Probl. Eng. 4. https://doi.org/10.1155/2012/386214.

Yun, T.M., Puspasari, I., Tasirin, S.M., Talib, M.Z.M., Daud, W.R.W., Yaakob, Z., 2013. Drying of oil palm frond particles in a fluidized bed dryer with inert medium. Chem. Ind. Chem. Eng. Q. 19, 593–603.

Zzaman, W., Biswas, R., Hossain, M.A., 2021. Application of immersion pretreatments and drying temperatures to improve the comprehensive quality of pineapple (*Ananas comosus*) slices. Heliyon 7, e05882. https://doi.org/10.1016/j.heliyon.2020.e05882e05882.